Dissociations of Gas-Phase CHClF and CHCl2 Radicals and Cations following Collisional Electron Transfer. A Variable-Time Neutralization−Reionization and ab Initio Study

ARTICLE *in* THE JOURNAL OF PHYSICAL CHEMISTRY · JANUARY 1996

Impact Factor: 2.78 · DOI: 10.1021/jp952416i

2 AUTHORS, INCLUDING:

František Tureček
University of Washington Seattle
166 PUBLICATIONS **2,475** CITATIONS

SEE PROFILE

Dissociations of Gas-Phase CHClF and $CHCl_2$ Radicals and Cations following Collisional Electron Transfer. A Variable-Time Neutralization−Reionization and ab Initio Study

Martin Sadílek and František Tureček*

Department of Chemistry, Box 351700, University of Washington, Seattle, Washington 98195-1700

Received: August 21, 1995; In Final Form: October 3, 1995[⊗]

Variable-time neutralization−reionization mass spectrometry is used to generate $CHClF^{\bullet}$ and $CHCl_2^{\bullet}$ radicals and to study their unimolecular dissociations within 0.4−4.1 μs. Loss of $Cl^{\bullet}$ is a major dissociation of $CHClF^{\bullet}$ following collisional neutralizations with di-*n*-butyl ether, chlorobenzene, di-*n*-butylamine, aniline, and *N*,*N*-dimethylaniline, which range from 0.28 eV endoergic to 1.7 eV exoergic in the same series. Loss of $H^{\bullet}$ also occurs, whereas loss of $F^{\bullet}$ and eliminations of HF and HCl are unimportant. Dissociations of $CHClF^{+}$ cations following collisional reionization of $CHClF^{\bullet}$ show eliminations of HF and HCl and losses of $F^{\bullet}$ and $Cl^{\bullet}$ whose rate parameters depend on the nature of the neutralization target. Both $CHCl_2$ radicals and ions undergo elimination of HCl and loss of $Cl^{\bullet}$ whose rate parameters are distinguished by the variable-time measurements. Ab initio calculations at the G2(MP2) level of theory give the bond dissociation energies for C−H, C−Cl, and C−F in $CHClF^{\bullet}$ as 307, 333, and 465 kJ mol^{-1}, respectively. Eliminations of HCl and HF have the lowest thermochemical thresholds, 217 and 225 kJ mol^{-1}, respectively, but overcome activation barriers. Franck−Condon effects in fast electron transfer are calculated to deposit 34 and 91 kJ mol^{-1} in the vertically formed $CHClF^{\bullet}$ and $CHClF^{+}$, respectively.

Introduction

The chemistry of hydrochlorofluorocarbons (HCFC) has been studied extensively in the past few years to elucidate decomposition processes by which these compounds are depleted in the troposphere and stratosphere.[1] Hydrogen atom abstraction by reaction with hydroxyl radical is considered to be an important pathway of HCFC removal in the troposphere,[2] while photolytic cleavage of the C−Cl bond is thought to be the main dissociation channel in the stratosphere.[3]

A topic of particular importance that has not been addressed widely is the high-energy chemistry of HCFC pertinent to their photolysis in the upper stratosphere and the stratopause. Absorption of short-wavelength solar radiation, e.g. a Lyman-α series photon of 983.8 kJ mol^{-1} energy, produces the HCFC molecule in a high Rydberg state,[4] causing exothermic dissociation by bond cleavages as indicated for $CHCl_2F$ in eqs 1−3.

$$CHCl_2F \rightarrow {}^{\bullet}CHClF + Cl^{\bullet} \qquad \Delta H_r = 297 \text{ kJ mol}^{-1} \quad (1)$$

$$\rightarrow {}^{\bullet}CCl_2F + H^{\bullet} \qquad \Delta H_r = 426 \text{ kJ mol}^{-1} \quad (2)$$

$$\rightarrow {}^{\bullet}CHCl_2 + F^{\bullet} \qquad \Delta H_r = 468 \text{ kJ mol}^{-1} \quad (3)$$

An important consequence is that the $CHClF^{\bullet}$ radicals formed by the least endothermic dissociation in eq 1 may possess enough energy to undergo further unimolecular dissociations such as loss of $Cl^{\bullet}$ of an estimated[5] $\Delta H_r = 335$ kJ mol^{-1}, or elimination of hydrogen chloride of an estimated $\Delta H_r = 268$ kJ mol^{-1}. 1,2-Elimination of hydrogen chloride from chemically activated HCFC molecules has been observed in the gas phase.[6]

While both the primary and the secondary dissociations of photoexcited HCFC molecules are thermochemically possible, their kinetics may vary substantially. HCFC radicals formed by photolysis may retain only a fraction of the original excitation energy,[6] in which case their unimolecular dissociations may be slow enough to compete with collisional cooling. The kinetics of HCFC radical unimolecular dissociations is therefore of importance for our understanding of the atmospheric chemistry of HCFC.[7] Gaseous $CHClF^{\bullet}$ radicals have been generated previously by hydrogen abstraction from CH_2ClF by fluorine atoms, and their photoelectron spectrum[8] and multiphoton ionization[9] have been studied in detail. $CHClF^{+}$ ions have been generated and studied in a matrix.[10]

In this paper we study gas-phase dissociations of two HCFC-related radicals, $CHClF^{\bullet}$ and $CHCl_2^{\bullet}$, and their corresponding cations $CHClF^{+}$ and $CHCl_2^{+}$ under strictly wall-less conditions using the recently introduced technique of variable-time neutralization−reionization mass spectrometry.[11] In this technique, the radicals are produced from their corresponding cation precursors of kiloelectronvolt kinetic energy by collisional electron transfer from a thermal gaseous organic molecule. Following electron transfer, unimolecular dissociations of the intermediate radicals are observed over a time interval, which is varied stepwise within 0.4−4.1 μs. The products of neutral dissociations are reionized to cations and analyzed by mass spectrometry. Dissociations of the reionized species are also observed on a variable time scale and deconvoluted from those of the neutral intermediates.[11]

Owing to the short interaction time in the glancing collision, estimated as $<10^{-14}$ s,[12] the neutralization event can be viewed as a vertical electron transfer. The internal energy deposited in the nascent radical typically does not exceed a few electronvolts and depends on several factors. Franck−Condon effects[12] are important in vertical neutralization of cations whose radical counterparts differ substantially in their equilibrium geometry.[13] The energy balance $\Delta E = RE_v(\text{ion}) - IE_v(\text{target})$, where RE_v and IE_v are the vertical ion recombination energy and target ionization energy, respectively, affects excitation of the fast neutrals, especially when ΔE is positive by several electronvolts.[14] Finally, the chemical nature of the target atom or molecule has been found empirically to have an effect on neutral excitation,[11b] although the mechanism of energy transfer is not well understood at present.[15]

[⊗] Abstract published in *Advance ACS Abstracts,* December 15, 1995.

0022-3654/96/20100-0224$12.00/0

We study the effects of collisional energy transfer in neutralizations with five organic molecules, where the charge transfer ranges from near thermoneutral ($\Delta E \sim 0$) to exoergic ($\Delta E > 0$). We also investigate the effects of the precursor cation internal energy on the radical dissociations. Ab initio calculations at the Gaussian 2(MP2) level of theory[16] are used to assess the thermochemistry of neutral and ion dissociations and locate some relevant transition states.

Experimental Part

The measurements were carried out on a tandem quadrupole acceleration−deceleration mass spectrometer described previously.[11,17] Chloroform (Baker) and difluorochloromethane (Matheson Halocarbon 22, 99.8%) were introduced into the ion source from a heated glass inlet system maintained at 60 °C; the sample intake was regulated by a fine metering valve to achieve a $(4-5) \times 10^{-6}$ Torr pressure in the ion source. Precursor ions were generated by electron-impact ionization; typical ionization conditions were as follows: electron energy, 70 eV; emission current, 400 μA; ion source potential, 80 V; ion source temperature, 180 °C; repeller potential, 0−2 V. For charge-exchange ionization, pure nitrogen was admitted in a tight chemical ionization ion source and ionized with 70-eV electrons. The optimum N_2 pressure was 2×10^{-4} Torr as measured on the intake of the ion source diffusion pump, corresponding to an estimated pressure of 0.2−0.3 Torr in the ionization chamber. The $N_2^{\bullet+}$ ions were titrated in the ion source by admitting difluorochloromethane at 4×10^{-6} Torr partial pressure. The precursor ions obtained by either ionization were passed through a quadrupole mass filter operated in the radio-frequency-only mode and floated at 40−60 V, accelerated to the total kinetic energy of 8220 eV and neutralized in a collision cell (cell I) floated at the acceleration voltage (−8140 V). Gaseous di-*n*-butyl ether (Aldrich), di-*n*-butylamine (Eastman Kodak), chlorobenzene, aniline, or *N*,*N*-dimethylaniline (Baker) was admitted from a heated glass manifold to a differentially pumped collision cell at pressures such as to achieve 70% transmittance of the precursor ion beam. The ions and neutrals were allowed to drift to a differentially pumped four-segment lens (the conduit),[11] where the ions were reflected by the first segment floated at +200 V and a fraction of the neutral species were reionized by collisions with oxygen at a pressure adjusted such as to achieve 70% transmittance of the precursor ion beam. The ions formed in the conduit were decelerated to ~80 eV kinetic energy, energy-filtered, and analyzed by a quadrupole mass filter operated at unit mass resolution. The potentials on the conduit segments, the deceleration lens, and the quadrupole mass filter were scanned in link to achieve mass-to-charge selection of both the precursor and product ions. The acceleration, deceleration, and all focusing potentials were tuned daily to maximize the ion current of reionized $CS_2^{\bullet+}$.

The variable-time measurements were carried out for four potential settings on the conduit segments as described previously,[11] corresponding to minimum neutral lifetimes of 0.46, 1.26, 2.08, and 2.88 μs for $CHCl_2^{\bullet}$ and 0.41, 1.14, 1.86, and 2.59 μs for $CHClF^{\bullet}$. $^{+}NR^{+}$ spectra were also obtained for reionization with oxygen in a downbeam collision cell (cell II) floated at the deceleration potential, corresponding to neutral lifetimes of 4.6 and 4.1 μs for $CHCl_2^{\bullet}$ and $CHClF^{\bullet}$, respectively. A total of 40−60 scans were typically accumulated at a scan rate of 1 mass unit/s and 75 data points per mass unit. Averaged ion intensities from integrated peak areas were used as input for kinetic calculations as described previously.[11] The calculated ratios of daughter to parent ion intensities were fitted against the experimental values from the variable-time measurements using phenomenological rate parameters[11] to minimize residual sums of squares. The other parameters needed in these calculations were the relative reionization efficiencies of the parent and daughter neutral species. These were estimated from correlated ionization cross sections[18] as discussed below.

The linked-scan mode may result in interferences due to transmission of reionized products from precursor ions of close *m/z* values.[19] For example, the fragmentations of precursor ions or neutrals of 8220 eV kinetic energy, $CH^{35}ClF \rightarrow {}^{35}Cl$ and $CH^{37}ClF \rightarrow {}^{37}Cl$, form the chlorine isotopes with 4294 and 4408 eV kinetic energy, respectively, so that the corresponding peak maxima are resolved by the energy filter.[17] However, if the fragmentations are accompanied by kinetic energy release *T*, the kinetic energy width of the $^{37}Cl^{+}$ peak at *m/z* 37 from the $CH^{37}ClF^{+}$ precursor at *m/z* 69 is given by eq 4.[20]

$$\Delta(eU_{dec}) = 4 \times (37/69) \times 8220[T \times (69 - 37)/(37 \times 8220)]^{1/2} = 180.85\sqrt{T} \quad (4)$$

Hence, for a nonzero *T*, a fraction of the $^{37}Cl^{+}$ ions from the $CH^{37}ClF^{+}$ precursor will have kinetic energies within the transmission window for an apparent *m/z* 67 → *m/z* 37 dissociation (4539 ± 25 eV) and appear as artifacts in the spectrum. For a Gaussian distribution of kinetic energy release and $T \geq 500$ meV (fwhm), more than 5% of $^{37}Cl^{+}$ is calculated to be cotransmitted and appear in the spectrum, as indeed observed (see below).

Collisionally activated dissociation (CAD) mass spectra were obtained on a Kratos Profile HV-4 double-focusing mass spectrometer of a forward geometry, in which the electrostatic sector (E) precedes the magnet (B). Collisions with oxygen were monitored in the first field-free region at a pressure to achieve 70% transmittance of the ion beam. The spectra were obtained by scanning E and B simultaneously while maintaining a constant B/E ratio (B/E linked scan).[19]

Calculations

Standard ab initio calculations were carried out using the Gaussian 92[21] suite of programs. Geometries were optimized using the 6-31G(d,p) basis set at two levels, Hartree−Fock (HF), and employing all-electron Møller−Plesset perturbation theory[22] truncated at second order, MP2(FULL)/6-31G(d,p), to estimate the correlation energy. Spin-unrestricted (UHF) wave functions were used for radicals and cation radicals. The unprojected $\langle S^2 \rangle$ values were within 0.75−0.77, indicating negligible spin contamination. Spin annihilation methods[23] further reduce the $\langle S^2 \rangle$ values; however, the corrections due to spin projection[24] to the approximated QCISD(T)/6-311+G(3df,2p) energies were <1 mhartree (< 2.6 kJ mol^{-1} or 0.027 eV) for all radicals under study. Calculations of radical transition states occasionally experienced SCF convergence problems, in which case Baczkay's quadratic convergence procedure was used.[25] Harmonic vibrational frequencies for $CHClF^{\bullet}$ and $CHClF^{+}$ were calculated with HF/6-31G(d,p) and scaled by 0.893.[26] The other vibrational frequencies were obtained with MP2(FULL)/6-31G(d,p) and scaled by 0.93. The frequencies were used to calculate zero-point vibrational energies and 298 K enthalpies, the latter within the rigid-rotor harmonic oscillator (RRHO) model. Improved energies were obtained from single-point calculations at the MP2/6-311+G(3df,2p)[16] and QCISD(T)/6-311G(d,p)[27] levels of theory using the MP2(FULL)/6-31G(d,p) geometries. The single-point energies were combined according to eq 5 to approximate QCISD(T)/6-311+G(3df,2p) calculations similar to the G2(MP2) scheme.[16] Empirical isogyric corrections

TABLE 1: Vertical Ionization Energies and Polarizabilities of Neutralization Targets and $^{+}NR^{+}$ Efficiencies for $CHClF^{+}$ and $CHCl_2^{+}$

species	IE_v (eV)[a]	α (Å^3)[b]	NR efficiency[c] × 10^5 $CHFCl^+$	NR efficiency[c] × 10^5 $CHCl_2^+$
di-*n*-butyl ether	9.44	17.2	4 ± 2	
chlorobenzene	9.10	12.3	7 ± 3	
di-*n*-butylamine	8.45	16.8[d]	13 ± 6	12
aniline	8.00	12.1	16 ± 11	40
N,*N*-dimethylaniline	7.45	16.2	18 ± 8	
$CHClF^{\bullet}$	9.16			
$CHCl_2^{\bullet}$	8.54			

[a] All data from ref 5. [b] From ref 43. [c] Defined as $\sum I_{NR}/I_0$, where $\sum I_{NR}$ is the sum of NR ion intensities and I_0 is the intensity of the precursor ion. [d] Estimated from the refractive index from ref 43.

inherent to the G2(MP2) scheme[16] cancel out in the isodesmic and isogyric reactions used to evaluate neutral and ion thermochemistry.

$$E\{\text{QCISD(T)/6-311+G(3df,2p)}\} \approx E\{\text{QCISD(T)/6-311G(d,p)}\} + E\{\text{MP2/6-311+G(3df,2p)}\} - E\{\text{MP2/6-311G(d,p)}\} \quad (5)$$

Results

Formation of $CHClF^{\bullet}$. $CHClF^+$ precursor ions were prepared by dissociative ionization of $CHClF_2$ according to eq 6 or 7 at 70 eV electron energy, which gives about 20% of $CHClF^+$ at *m/z* 67 relative to the CHF_2^+ base peak. These $CHClF^+$ ions were produced at $<10^{-5}$ Torr partial pressure of $CHClF_2$, such that their formation be mainly due to unimolecular dissociations. $CHClF^+$ ions were also generated by charge-exchange ionization of $CHClF_2$ with $N_2^{\bullet+}$ at 0.2−0.3 Torr of nitrogen gas (eq 8).

$$CHClF_2 + e^- \rightarrow CHClF^+ + F^{\bullet} + 2e^- \quad (6)$$

$$\rightarrow CHClF^+ + F^- + e^- \quad (7)$$

$$CHClF_2 + N_2^{\bullet+} \rightarrow CHClF^+ + F^{\bullet} + N_2 \quad (8)$$

$CHClF^+$ ions prepared by electron impact likely have a broad distribution of internal energies limited by the lowest dissociation threshold at 346 kJ mol^{-1} (vide infra). By contrast, charge-transfer (CT) ionization with $X(^2\Sigma^+_g)N_2^{\bullet+}$ generates the C + D states of $CHClF_2^{\bullet+}$,[28] which lie ca. 3 eV above the $X(^2A'')$ ground state. From the energy balance of eq 8,[5,28] it follows that $CHClF^+$ ions prepared by dissociative CT ionization can receive a maximum of 197 kJ mol^{-1}. A part of this available energy can be dissipated by the 40−50 collisions with the nitrogen gas that the ions undergo before leaving the ion source. $CHClF^+$ has a low heat capacity, as calculated from the RHF/6-31G(d,p) harmonic vibrational frequencies[29] scaled by 0.893, e.g., 469 (a′), 931 (a′), 979 (a″), 1304 (a′), 1467 (a′), and 3043 (a′) cm^{-1}, with the use of the RRHO approximation. A fully thermalized ion is calculated to contain on average only 18.1 kJ mol^{-1} at the ion source temperature of 180 °C.

The ions were neutralized with a series of gaseous targets of vertical ionization energies (IE_v) that bracket the experimental IE_v of $CHClF^{\bullet}$ (Table 1). Neutralization−reionization efficiencies, defined as the sum of reionized ion intensities relative to that of the $CHClF^+$ precursor ion, $\sum I_{NR}/I_0$, were determined for all the neutralization targets at 8220 keV collision energy (Table 1). NR efficiencies were also measured for some of the fragments as discussed below. The NR efficiencies for $CHClF^+$ roughly increase with the decreasing IE_v of the neutralization target gases, while no maximum is observed for neutralization with chlorobenzene. No obvious dependence on the target polarizabilities is observed. This shows that long-range attraction due to the ion-induced dipole potential (α/R^4) is unimportant in these collisions at kiloelectronvolt laboratory kinetic energies.[30]

The overall NR spectra (Table 2), corresponding to neutral lifetimes of 4.1 μs, are relatively insensitive to the nature of the neutralization gas. Mildly endoergic neutralization with di-*n*-butyl ether as well as exoergic neutralization with *N*,*N*-dimethylaniline results in the formation of a significant fraction of stable $CHClF^{\bullet}$ that are detected as survivor ions at *m/z* 67 (Table 2). Major dissociation channels correspond to the formation of the complementary CHF^+ (*m/z* 32) and Cl^+ (*m/z* 35) and elimination of HCl to form CF^+ at *m/z* 31. The other dissociations are the loss of $H^{\bullet}$ (*m/z* 66), loss of $F^{\bullet}$ (*m/z* 48), and elimination of HF (*m/z* 47). The complementary fluorine fragments are very weak. The F^+ ion, which is complementary to $CHCl^{\bullet+}$, represents only 0.1−0.6% relative intensity, and the $HF^{\bullet+}$ ion, complementary to CCl^+, is at the background noise level, which is <2% of the F^+ intensity. The NR spectrum obtained by neutralization with di-*n*-butylamine shows more extensive dissociation, resulting in an enhanced formation of $HCl^{\bullet+}$, Cl^+, and CF^+ (Table 2).

A substantial effect on NR relative ion intensities is observed for the ions prepared by CT ionization (Table 2). For the three neutralization target gases used, the CT-NR spectra show about 50% higher relative intensities of the survivor ions than do the NR spectra of $CHClF^+$ from electron impact ionization. Changes are also observed in the fragment ion relative intensities; e.g., the $[CHCl^{\bullet+}]/[CCl^+]$ and $[CHF^{\bullet+}]/[CF^+]$ ratios are greater for the ions from charge transfer ionization. By contrast, the $[Cl^+]/[CHF^{\bullet+}]$ ratios for the complementary fragments change only little (Table 2).

To assess the extent of ion dissociations following reionization, the $^{+}NR^{+}$ spectra are compared with the collisionally activated dissociation (CAD) spectrum of $CHClF^+$ (Table 2). The latter shows dominant formations of $CHF^{\bullet+}$ and CF^+, while those of Cl^+ and $HCl^{\bullet+}$ are relatively less abundant. Loss of $F^{\bullet}$ and elimination of HF also occur upon CAD. A complementary experiment was also carried out in which $CHClF^+$ was excited by collisions with helium,[31] which is a very inefficient electron donor.[32] The ion products were deflected away, and the neutral fragments were reionized after 4.1 μs. This CAD/reionization spectrum[33] showed predominant peaks of Cl^+ and $HCl^{\bullet+}$ in a 3.6/1 ratio, confirming the formation of their corresponding neutrals by ion dissociations.

Formation of $CHCl_2^{\bullet}$. The $CHCl_2^+$ precursor ion was generated by dissociative electron impact ionization of chloroform at 70 eV. Ion dissociations were assessed through the CAD spectrum of $CHCl_2^+$ (Figure 1b), which shows CCl^+ and $CHCl^{\bullet+}$ as the predominant fragments, whereas the peak of Cl^+ is less abundant. The $CHCl_2^+$ ions were neutralized by mildly exothermic electron transfer from di-*n*-butylamine ($\Delta IE_v = 0.09$ eV) and aniline ($\Delta IE_v = 0.54$ eV). The NR spectrum obtained with di-*n*-butylamine (Figure 1a) shows a substantial survivor ion of $CHCl_2^+$ at *m/z* 83. Hence, vertical electron transfer produces a fraction of stable $CHCl_2^{\bullet}$ radicals of a 4.6 μs lifetime. The major fragments observed in the spectrum are CCl^+ at *m/z* 47 due to loss of HCl and the complementary $CHCl^{\bullet+}$ and Cl^+ at *m/z* 48 and 35, respectively. $HCl^{\bullet+}$, $CCl_2^{\bullet+}$, $Cl_2^{\bullet+}$, CH^+, and $C^{\bullet+}$ represent minor dissociation products. Small peaks of ^{37}Cl-containing ions due to imperfect precursor ion selection appear at *m/z* 37, 49, and 50. NR efficiencies for $CHCl_2^+$ were measured for di-*n*-butylamine and aniline and showed an

TABLE 2: $^+NR^+$ Spectra of $CHClF^+$ Obtained by Neutralization with Chlorobenzene (a), Di-*n*-butyl Ether (b), Di-*n*-butylamine (c), Aniline (d), and *N*,*N*-Dimethylaniline (e) and CAD (O_2, 70% T) Spectrum

		relative intensity[a,b]								
		70-eV EI ionization					charge-transfer ionization			
species	*m/z*	a	b	c	d	e	a	d	e	CAD[c]
CHClF	67	22.1	21.8	16.4	22.6	21.7	33.7	33.6	34.3	
CClF	66	4.5	4.5	3.4	2.5	3.5	4.6	4.9	4.5	(29)[d]
CHCl	48	3.6	3.8	3.0	2.0	2.5	4.4	4.4	5.0	5.3
CCl	47	8.6	9.3	9.2	7.9	8.2	9.2	8.6	9.0	9.9
HCl	36	3.8	3.7	4.3	2.6	3.3	3.7	2.1	2.2	0.9
Cl	35	16.2	17.6	19.9	18.3	17.8	13.7	13.3	13.3	5.9
CHF	32	16.8	15.9	16.9	17.6	17.0	15.0	15.7	14.5	47.6
CF	31	22.9	22.3	26.2	26.2	25.3	15.3	16.8	16.1	30.4
F	19	0.6	0.3	0.2	0.1	0.2	0.7	0.2	0.2	
CH	13	0.5	0.4	0.2	0.1	0.2	0.3	0.1	0.4	
C	12	0.4	0.4	0.3	0.2	0.3	0.3	0.3	0.4	

[a] Relative to the sum of reionized ion intensities measured as integrated peak areas. [b] All data obtained at 70% precursor ion transmittance in both neutralization and reionization. [c] Collisions with O_2 at 70% precursor ion beam transmittance. [d] Possibly affected by artifacts due to B/E linked scan.

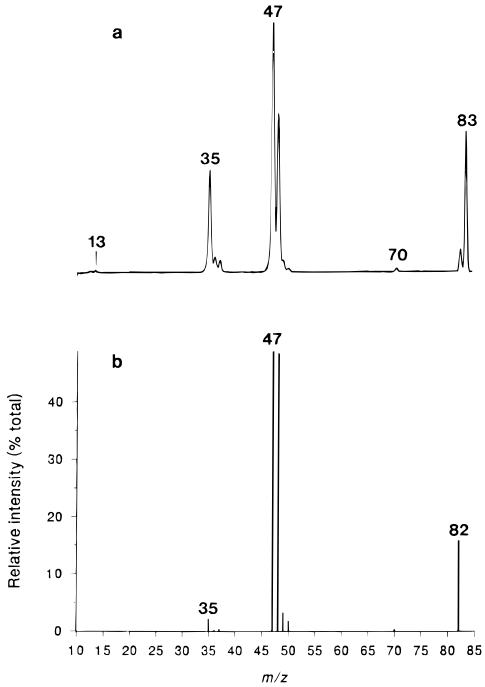

Figure 1. (a) Neutralization−reionization mass spectrum of $CHCl_2^+$, $(n\text{-}C_4H_9)_2NH$ (70% T)/O_2 (70% T). (b) Collisionally activated dissociation spectrum of $CHCl_2^+$, O_2, 70% ion beam transmittance (T).

increase with the increasing neutralization exoergicity, in keeping with the results obtained for $CHClF^+$ (Table 1).

Variable-Time Measurements. Variable-time NR spectra were measured at four different potential settings on the reionization conduit.[11] In this way reionized ions are selected corresponding to four combinations of neutral (τ_N) and ion (τ_i) lifetimes, such that the total drift time $\tau = \tau_N + \tau_i$ remains constant. Kinetic equations[11] were solved to fit the experimental relative intensities with a double-exponential model[11] to provide rate parameters for dissociations of $CHClF^\bullet$, $CHCl_2^\bullet$, and their reionized counterparts $CHClF^+$ and $CHCl_2^+$ as summarized in Table 3. Due to the reionization step, the measured ion relative intensities must be corrected for the different reionization yields of the precursor radicals and their dissociation products.[34] Reionization yields of organic molecules and radicals are mostly unknown[34] and difficult to measure.[34−36] We presume that collisional reionization at kiloelectronvolt kinetic energies is qualitatively similar to electron impact ionization at nonthreshold electron energies in that *relative* electron impact ionization cross sections can be used to approximate *relative* reionization efficiencies.[37] The electron impact ionization cross sections are estimated from the atomic increments for C, H, Cl, and F according to Fitch and Sauter.[18] Furthermore, the range of neutral and ion lifetimes used (0.41−2.59 μs for CHClF) sets limits for the rate constants of observable dissociations, e.g., 7.5×10^6 s^{-1} for 95% dissociation at the shortest time and 2×10^4 s^{-1} for 5% dissociation at the longest time. Hence, fast dissociations ($k > 10^7$ s^{-1}) of highly excited radicals are unresolved. We considered such fast reactions by introducing into the kinetic schemes variable fractions (0−50%) of CHClF radicals that dissociated immediately after neutralization and were reionized to products. These calculations showed that the experimental product ratios could be fitted best with very low fractions of fast dissociating radicals (0−5%), and the fits became gradually worse when the fractions were increased. This indicates that most of the neutral dissociations observed can be assigned rate constants in the 10^4−10^6 s^{-1} range.

The rate parameters in Table 3 reveal several features that are not distinguished by the overall NR mass spectra of $CHClF^+$. Loss of the fluorine atom is due chiefly to ion dissociations, which become significant for neutralization with di-*n*-butylamine. Similarly, elimination of hydrogen fluoride is due to ion dissociations following reionization with the rate parameters roughly increasing with the neutralization exoergicity. The formations of CHF and CF show apparent contributions from both neutral and ion dissociations for neutralizations with di-*n*-butyl ether through aniline. The most exoergic neutralization with *N*,*N*-dimethylaniline results in somewhat greater rate parameters for the formations of CHF and CF from neutral $CHClF^\bullet$, whereas the rate parameters for ion dissociations do not exceed those obtained from the endoergic or less exoergic neutralizations. The rate parameters for the formation of Cl^+ show predominance of ion dissociations. This is somewhat surprising in view of the high endothermicity for the formation of Cl^+ (Table 4). It is possible, however, that Cl^+ can be formed convergently by competitive and consecutive dissociations, the latter of which are not treated explicitly by the kinetic scheme.[11]

The rate parameters for eliminations of $Cl^\bullet$, and HCl from the $CHCl_2$ system depend on the neutralization gas. Neutralization with di-*n*-butylamine, which is almost thermoneutral (Table 1), results in similar rate parameters for dissociations of neutral $CHCl_2^\bullet$ and reionized $CHCl_2^+$ (Table 3). By contrast, mildly exoergic neutralization with aniline results in decreased rate parameters for dissociations of reionized $CHCl_2^+$.

Thermochemistry of $CHClF^\bullet$ and $CHClF^+$ Dissociations. In order to discuss the kinetic data, threshold energies for the

TABLE 3: Rate Parameters for Dissociations of $CHClF^{\bullet}$, $CHClF^{+}$, $CHCl_2^{\bullet}$, and $CHCl_2^{+}$ [a]

	neutralization target									
	$(n\text{-}C_4H_9)_2O$		C_6H_5Cl		$(n\text{-}C_4H_9)_2NH$		$C_6H_5NH_2$		$C_6H_5N(CH_3)_2$	
reactant/products	k_N	k_i	k_N	k_i	k_N	k_i	k_N	k_i	k_N	k_i
$CHClF^{\bullet}$										
CHCl	0.03	0.08	0.07	0.10	0.02	0.25	0.006	0.11	0.00	0.04
CCl	0.09	0.16	0.13	0.38	0.10	0.51	0.05	0.48	0.01	0.66
CHF	0.32	0.30	0.44	0.34	0.34	0.59	0.36	0.34	0.41	0.28
CF	0.42	0.65	0.58	0.55	0.56	0.72	0.56	0.53	0.63	0.41
HCl	0.04	0.20	0.08	0.23	0.10	0.19	0.00	0.12	0.03	0.04
Cl	0.29	0.65	0.42	0.52	0.33	0.95	0.36	0.47	0.35	0.58
$CHCl_2^{\bullet}$										
CHCl					0.36	0.36	0.39	0.24		
CCl					0.50	0.50	0.51	0.29		
Cl					0.46	0.37	0.47	0.20		

[a] Rate parameters (10^6 s^{-1}) for neutral (k_N) and ion (k_i) dissociations.

TABLE 4: Thermochemical Data for $CHClF^{\bullet}$, $CHClF^{+}$, $CHCl_2^{\bullet}$, and $CHCl_2^{+}$ Dissociations

reactant		products	$\Delta H_{r,298}$[a]	products	$\Delta H_{r,298}$[a]
$CHClF^{\bullet}$	→	$CCl^{\bullet} + HF$	217		
		$CF^{\bullet} + HCl$	267		
		$CClF + H^{\bullet}$	302		
		$CHF + Cl^{\bullet}$	335		
		$CHCl + F^{\bullet}$	481		
$CHClF^{+}$	→	$CCl^{+} + HF$	227	$CCl^{\bullet} + HF^{\bullet+}$	683
		$CF^{+} + HCl$	297	$CF^{\bullet} + HCl^{\bullet+}$	648
		$CHF^{\bullet+} + Cl^{\bullet}$	498	$CHF + Cl^{+}$	737
		$CHCl^{\bullet+} + F^{\bullet}$	581	$CHCl + F^{+}$	1313
		$CHCl^{\bullet+} + H^{\bullet}$	601	$CClF + H^{+}$	765
$CHCl_2^{\bullet}$	→	$CCl^{\bullet} + HCl$	184		
		$CCl_2 + H^{\bullet}$	272		
		$CHCl + Cl^{\bullet}$	310		
		$CH + Cl_2$	490		
		$CHCl + F^{\bullet}$	481		
$CHCl_2^{+}$	→	$CCl^{+} + HCl$	240	$CCl^{\bullet} + HCl^{+}$	611
		$CHCl^{\bullet+} + Cl^{\bullet}$	456	$CHCl + Cl^{+}$	758
		$CCl_2^{\bullet+} + H^{\bullet}$	469	$CCl_2 + H^{+}$	782
		$CH^{+} + Cl_2$	711	$CH^{\bullet} + Cl_2^{\bullet+}$	795

[a] Calculated from the thermochemical data from ref 5.

radical and ion dissociations are needed. The available thermochemical data, which are based on experimental or estimated heats of formation, are summarized in Table 4. To obtain a consistent set including activation energies for eliminations of HF and HCl, additional energy data were obtained from the QCISD(T)/6-311+G(3df,2p) total energies (eq 2) and zero-point and enthalpy corrections, as summarized in Table 5. Table 6 gives the 298 K reaction enthalpies, which are further compared with the experiment-based data in Table 4. Lowest singlet states were obtained throughout for closed-shell species. Triplet energies were checked with MP2(FULL)/6-31G(d,p) calculations for CClF, CHF, CCl^{+}, and CF^{+} and found to be higher than those for the singlets (Table 5).

With ion dissociations, elimination of hydrogen fluoride has the lowest thermochemical threshold, which was calculated at 256 kJ mol^{-1} above $CHClF^{+}$ (Table 6). The experimental estimate is substantially lower (Table 4). The elimination of HF overcomes an activation barrier calculated at 365 kJ mol^{-1} above $CHClF^{+}$ and 109 kJ mol^{-1} above the products. The transition state geometry is given in Chart 1. Elimination of hydrogen chloride is calculated to require 281 kJ mol^{-1} at the thermochemical threshold, which is in a fair agreement with the experimental estimate (Table 4). An activation barrier for HCl elimination is found 346 kJ mol^{-1} above $CHClF^{+}$ and 65 kJ mol^{-1} above the products. Hence, elimination of HCl is the lowest-energy dissociation of $CHClF^{+}$. The transition states for both eliminations are planar, and the reaction coordinate in the vicinity of the saddle point corresponds to hydrogen atom motion nearly parallel with the C−F or C−Cl bond (Chart 1). In spite of the activation barriers, the transition state energies for HF and HCl eliminations are substantially lower than the lowest threshold for direct bond cleavage in $CHClF^{+}$ by loss of $Cl^{\bullet}$ (Tables 4 and 6, Figure 2), indicating that the eliminations should be kinetically competitive with the losses of $F^{\bullet}$, $Cl^{\bullet}$, and $H^{\bullet}$.

The calculations further locate two intermediates in the elimination reactions (Chart 1). Elimination of HF may proceed through an ion−molecule complex[38] ($HF\cdot\cdot CCl^{+}$, Chart 1 and Figure 2), which is stabilized by 42 kJ mol^{-1} against dissociation to HF and CCl^{+}. An analogous $HCl\cdot\cdot CF^{+}$ complex (Chart 1) is found to be stabilized by 71 kJ mol^{-1} against dissociation to HCl and CF^{+}, and it may represent an intermediate in the HCl elimination. However, because of the activation barriers separating $CHClF^{+}$ from the $HF\cdot\cdot CCl^{+}$ and $HCl\cdot\cdot CF^{+}$ complexes, the latter ions formed by classical unimolecular isomerizations (i.e., without tunneling) of $CHClF^{+}$ will have sufficient energies to dissociate on the microsecond time scale (Figure 2). This leads to the conclusion that nondissociating $CHClF^{+}$ ions formed from $CHClF_2$ and sampled for collisional neutralization cannot interconvert with other isomers and must retain the bond connectivity of the chlorofluoromethyl cation. An interesting question is whether the $HCl\cdot\cdot CF^{+}$ and $HF\cdot\cdot CCl^{+}$ complexes could interconvert through another pathway, e.g., via a proton transfer between Cl and F that would avoid $CHClF^{+}$ as an intermediate. Such an isomerization has not been studied; it is pertinent to note that analogous 1,3-proton transfers proceeding through four-membered cyclic transition states have substantial activation barriers.[39]

The potential energy surface for loss of $F^{\bullet}$ and elimination of HF from $CHClF^{\bullet}$ radicals has been investigated in some detail with UMP2(FULL)/6-31G(d,p) calculations. Loss of $F^{\bullet}$ is continuously endothermic along the C−F reaction coordinate, whereby the F atom departs at ∼108° angle with respect to the H−C−Cl plane. The threshold for $F^{\bullet} + (^1A')HCCl$ is calculated by G2(MP2) at 465 kJ mol^{-1}, in fair agreement with experimental estimates (Table 4). An attack on the hydrogen atom in HCCl by free $F^{\bullet}$ proceeds almost collinearly with respect to the H−C bond ($\angle F-H-C \sim 175°$) and is continuously exothermic to form HF and $CCl^{\bullet}$ 240 kJ mol^{-1} below the reactants ($F^{\bullet}$ + HCCl) and 225 kJ mol^{-1} above $CHClF^{\bullet}$ (Table 6). The latter value is in good agreement with the experimental estimate (Table 4). Elimination of HF from $CHClF^{\bullet}$ proceeds through a saddle point interconnecting the troughs for the endothermic C−F bond fission and exothermic H abstraction by free $F^{\bullet}$ and shows significant C−F separation (Chart 1). The transition state is located at 306 kJ mol^{-1} above the reactant and 81 kJ mol^{-1} above the products (Table 6). This is

TABLE 5: Total ab Initio Energies, Zero-Point Vibrational Energies, and 298 K Enthalpy Corrections

species	total energy[a] MP2(FULL)/6-31G(d,p)	MP2/6-311+G (3df,2p)	MP2/6-311G(d,p)	QCISD(T)/6-311G(d,p)	QCISD(T)/6-311+G(3df,2p)	ZPVE[b,c]	$H_{298} - H_0$[b]
			Neutrals				
CHClF•	−597.737 500	−597.969 512	−597.829 678	−597.867 310	−598.007 144	44.5	11.3
CHClF•(VN)[d]		−597.957 402	−597.814 154	−597.850 918	−597.994 167		
TS(HF···CCl•)[e]	−597.606 290	−597.841 105	−597.700 531	−597.743 816	−597.884 391	27.2	12.3
CClF(^{1}A′)	−597.110 361	−597.340 752	−597.201 622	−597.241 877	−597.381 007	13.8	11.0
CClF(^{3}A″)	−597.061 460					14.1	11.1
	−597.062 979[f]						
CHCl(^{1}A′)	−498.054 616	−498.170 612	−498.089 340	−498.130 830	−498.212 102	28.8	10.2
CHF(^{1}A′)	−138.044 600	−138.196 062	−138.115 697	−138.145 353	−138.225 718	31.4	10.0
CHF(^{3}A″)	−138.030 827					32.0	10.0
	−138.032 060[f]						
CCl•	−497.432 802	−497.542 367	−497.465 228	−497.504 435	−497.581 574	5.0	8.9
CF•	−137.430 894	−137.575 544	−137.499 855	−137.525 578	−137.601 267	7.5	8.7
HF	−100.196 700	−100.329 428	−100.267 141	−100.273 868	−100.336 155	23.3	8.7
HCl	−460.215 621	−460.298 760	−460.244 005	−460.263 311	−460.318 066	17.4	8.7
F•		−99.602 117	−99.554 171	−99.565 804	−99.613 751		6.2
Cl•		−459.633 378	−459.585 137	−459.603 286	−459.651 527		6.2
H•					−0.499 810		6.2
			Ions				
$CHClF^+$	−597.445 668	−597.667 088	−597.534 143	−597.571 077	−597.704 022	50.0	10.8
$CHClF^+$(VI)[g]		−597.627 712	−597.495 392	−597.537 066	−597.669 386		
TS(HF··CCl^+)[h]	−597.296 332	−597.517 175	−597.384 151	−597.424 310	−597.557 335	28.9	11.5
TS(HCl··CF^+)[i]	−597.291 028	−597.521 352	−597.387 903	−597.430 588	−597.564 037	27.4	12.0
HF··CCl^+	−597.348 222	−597.572 013	−597.443 715	−597.490 264	−597.618 562	34.8	16.0
HCl··CF^+	−597.353 607	−597.573 491	−597.444 683	−597.490 295	−597.619 102	31.9	15.7
CCl^+($^1\Sigma^+$)	−497.127 888	−497.225 027	−497.156 343	−497.196 722	−497.265 407	7.1	8.7
CCl^+($^3\Pi$)	−497.016 531						
	−497.020 296[f]						
CF^+($^1\Sigma^+$)	−137.113 960	−137.246 731	−137.178 122	−137.204 194	−137.272 804	10.1	8.7
CF^+($^3\Pi$)	−136.946 907						
	−136.948 082[f]						
$CHF^{\bullet+}$	−137.701 081	−137.838 292	−137.767 132	−137.790 658	−137.861 817	33.1	10.0

[a] In units of hartree, 1 hartree = 2625.5 kJ mol^{-1}. [b] In units of kJ mol^{-1}. [c] From HF/6-31G(d,p) harmonic frequencies scaled by 0.893 and MP2(FULL)/6-31G(d,p) frequencies scaled by 0.93. [d] Single-point energy on the optimized ion geometry. [e] Transition state for HF elimination. [f] After spin projection(ref 24). [g] Single-point energy on the optimized radical geometry. [h] Transition state for HF elimination. [i] Transition state for HCl elimination.

TABLE 6: Ab Initio Relative Enthalpies at 0 and 298 K[a,b]

species	$\Delta H_{r,0}$	$\Delta H_{r,298}$
Neutrals		
CHClF•	0	0
CHClF•(VN)[c]	34	34
HF + CCl•	219	225
TS(CHClF• → HF + CCl•)	305	306
HCl + CF•	211	217
CClF + H•	301	307
CHF + Cl•	328	333
CHCl + F•	460	465
Ions		
$CHClF^+$	0	0
$CHClF^+$(VI)[d]	91	91
HF··CCl^+	209	214
TS($CHClF^+$ → HF··CCl^+)	364	365
HCl··CF^+	205	210
TS($CHClF^+$ → HCl··CF^+)	345	346
CCl^+ + HF	249	256
CF^+ + HCl	274	281
$CHF^{\bullet+}$ + Cl•	505	509

[a] From QCISD(T)/6-311+G(3df,2p) energies (eq 5) and HF/6-31G(d,p) or MP2(FULL)/6-31G(d,p) zero-point and enthalpy corrections. [b] In units of kJ mol^{-1}. [c] By vertical neutralization of $CHClF^+$. [d] By vertical ionization of CHClF•.

comparable to the threshold for the lowest-energy cleavage of the C−H bond in CHClF•, which is calculated to require 307 kJ mol^{-1} in good agreement with the experimental datum (Table 4). Cleavage of the C−Cl bond is slightly more endothermic; its bond dissociation energy is calculated as 333 kJ mol^{-1} (Table 6), in excellent agreement with the experimental estimate (Table 4). The transition state for the elimination of HCl was not obtained because of problems with SCF convergence in the vicinity of the saddle point. Nonetheless, the calculations indicate an activation energy for the HCl elimination.

Effects of vertical electron transfer in neutralization and reionization are assessed through the Franck−Condon energies obtained as differences between the total energies of the optimized structures and those after attachment or removal of an electron (Table 5). Vertical neutralization of vibrationally relaxed $CHClF^+$, corresponding to all $v = 0$, is accompanied by deposition of 34 kJ mol^{-1} in the incipient radical (Table 6). Vertical ionization of relaxed CHClF• results in a deposition of 91 kJ mol^{-1} in the ion formed. These excitations in the vertically formed ion and radical are chiefly due to differences in the C−F and C−Cl bond lengths and the dihedral angle about the carbon atom. The relatively small Franck−Condon energy for vertical neutralization of $CHClF^+$ is consistent with excitation of the soft vibrational modes in CHClF•, e.g., the F−C−Cl scissor bend (387 cm^{-1}), the C−H out-of plane bend (757 cm^{-1}), and the C−F stretch (1158 cm^{-1}). By comparison, the inversion barrier in CHClF• has been calculated as 14 kJ mol^{-1},[9] which indicates that the planar deformation in vertically formed CHClF• contributes ca. 40% of the Franck−Condon energy.

The G2(MP2) ionization energies, including isogyric corrections,[16] show very good agreement with experimental data for CF•, which gives 9.11 eV from G2(MP2) versus 9.11 ± 0.01 eV,[40] and CCl•, which gives 8.80 eV from G2(MP2) versus 8.9 ± 0.2 eV.[41] The adiabatic ionization energy (IE_a) of CHClF•

Chart 1: Optimized Structures and Harmonic Vibrational Frequencies[a]

species	bond length[b]	angle[c]	uncorrected freq, cm^{-1}
$CHClF^+$(C_s)	C−H 1.087	H−C−F 116.62	RHF/6-31G(d): 525, 1043, 1096, 1460, 1642, 3406
	C−F 1.266	H−C−Cl 122.55	
	C−Cl 1.599		
HF··CCl^+	H−F 0.932	H−F−C 123.14	RHF/6-31G(d,p): 149, 184, 227, 329, 1266, 4364
	C−F 2.245	F−C−Cl 94.91	
	C−Cl 1.541	H−F−C−Cl 179.90	
HCl··CF^+(C_s)	H−Cl 1.281	H−Cl−C 95.31	RHF/6-31G(d,p): 134, 139, 255, 464, 1872, 3112
	C−Cl 2.331	Cl−C−F 102.63	
	C−F 1.201	H−Cl−C−F 180	
TS(HF··CCl^+)(C_s)	C−F 1.583	Cl−C−F 112.77	RHF/6-31G(d,p): i2170, 433, 665, 840, 1113, 2359
	C−H 1.329	H−F−C−Cl 180	
	H−F 1.149		
	C−Cl 1.561		
TS(HCl··CF^+)(C_s)	C−Cl 1.841	F−C−Cl 114.06	RHF/6-31G(d,p): i2257, 413, 447, 758, 1539, 1973
	H−Cl 1.486	H−Cl−C−F 180	
	C−H 1.372		
	C−F 1.240		
$CHClF^•$	C−H 1.080	H−C−F 113.81	UHF/6-31G(d,p): 434, 848, 941, 1298, 1439, 3371
	C−F 1.340	H−C−Cl 116.20	
	C−Cl 1.710	Cl−C−H−F 136.07	
TS(FH··$CCl^•$)	H−F 1.155	Cl−C−F 108.50	UHF/6-31G(d,p): i2147, 248, 613, 788, 943, 2505
	C−H 1.242	Cl−C−H−F 61.75	
	C−F 1.850		
	C−Cl 1.648		

[a] MP2(FULL)/6-31G(d,p) optimized structures. [b] Bond lengths in angstroms. [c] Bond and dihedral angles in degrees.

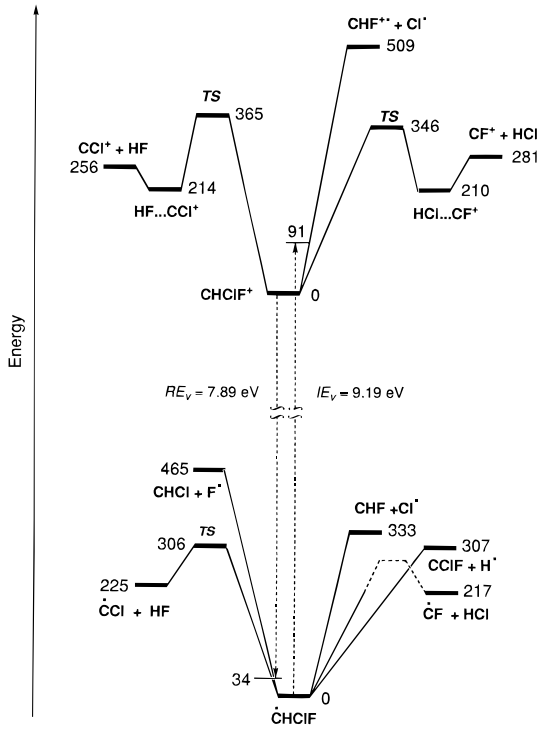

Figure 2. Potential energy diagram for dissociations of $CHClF^+$ and $CHClF^•$. The energy data are 298 K enthalpies from QCISD(T)/6-311+G(3df,2p) + ZPVE calculations.

has been estimated as 8.81 eV from the onset of the first band in the photoelectron spectrum of $CHClF^•$, which showed extensive vibrational progression indicating large Franck−Condon effects.[8] The G2(MP2) calculated value, $IE_a(CHClF^•) = 8.44$ eV, is lower than the experimental estimate. Hudgens and co-workers[9] calculated $IE_a(CHClF^•) = 8.37 \pm 0.05$ eV using MP2/6-311++G(d,p) energies for five charge-exchange (isogyric) reactions and noted the disagreement with the experimental estimate.[8,9] The reason for the rather large discrepancy between the calculated values and the experimental estimate is unclear. The G2(MP2) vertical ionization energy (IE_v) of $CHClF^•$ is somewhat larger than the experimentally assigned value (9.16 eV).[8] The latter is well reproduced by the QCISD(T)/6-311+G(3df,2p) calculations, which give $IE_v = 9.19$ eV without the isogyric correction. It is worth noting that the G2(MP2) calculated $IE_v = 9.32$ eV coincides with the position of the photoelectron band of $CHClF^•$ assigned to the $v' = 0-1$ transition.[8] Hence, the assignment of the accurate $IE_v(CHClF^•)$ from the present calculations remains ambiguous.

Discussion

The variable-time measurements allow one to distinguish unimolecular dissociations of the intermediate radicals from those of their reionized counterparts. It should be noted that each elementary neutral dissociation forms two products, whose rate parameters must correlate. Ideally, the rate parameters for each pair of complementary neutral fragments should be identical, but the values obtained from the measurements can be skewed by the estimates of the reionization efficiencies. In contrast, ion dissociations form cation−neutral pairs, in which the positive charge resides on the fragment of lower ionization energy,[42] corresponding to the ground electronic state of the cation−neutral system. Hence, the k_i values for complementary fragments do not correlate, unless the fragments have very similar ionization energies. Table 3 shows that the k_N of CHF and Cl correlate for all the neutralization targets used. Dissociation of the C−Cl bond in $CHClF^•$ is thus clearly established. By contrast, whereas the formation of CF shows a substantial k_N, the formation of its HCl counterpart does not. This indicates that $CHClF^•$ radicals do not eliminate HCl efficiently following neutralization. In order to explain the substantial k_N for the formation of CF^+, we assume contributions from consecutive dissociations, $CHClF^• \rightarrow CClF + H^•$, $CClF \rightarrow CF^• + Cl^•$ and $CHClF^• \rightarrow CHF + Cl^•$, $CHF \rightarrow CF^• + H^•$, as the sources of $CF^•$. These neutral dissociation paths are substantially endothermic, requiring 641 kJ mol^{-1} (Table 6), and thus should proceed competitively in the high-energy fraction of $CHClF^•$ only. By contrast, the ion dissociation $CClF^{•+} \rightarrow CF^+ + Cl^•$ is only 128 kJ mol^{-1} endothermic[5] and hence should proceed rapidly in reionized $CClF^{•+}$. This being the case, the neutral dissociation becomes the rate-limiting step in the overall reaction sequence, $CHClF^• \rightarrow CClF \rightarrow CClF^{•+}$

$\rightarrow CF^+$, and the formation of CF^+ will show a k_N value simulating that for the elimination of HCl. That loss of $Cl^\bullet$ from $CClF^{\bullet+}$ is facile is documented by the NR mass spectrum of the latter ion, which shows abundant CF^+(49.6%), survivor $CClF^{\bullet+}$ (14.6%), Cl^+ (29.2%), and weak CCl^+ (6.3%) and F^+ (0.3%).

The formations of CHCl and $CCl^\bullet$ due to loss of $F^\bullet$ and elimination of HF, respectively, show only small k_N values attesting to inefficient neutral dissociations by these channels. This is consistent with the very low fractions of reionized F^+ and $HF^{\bullet+}$ for which the k_N values could not be measured because of low ion intensities. Note that the formation of CCl by consecutive dissociations, $CHClF^\bullet \rightarrow CClF + H^\bullet$, $CClF \rightarrow CCl + F^\bullet$, requires $307 + 488 = 795$ kJ mol^{-1}, which hampers its occurrence in neutral dissociations.

Thermochemical data (Table 6) indicate that threshold energies for the losses from $CHClF^\bullet$ of $H^\bullet$ and $Cl^\bullet$ are comparable to the activation barrier for HF elimination. Kinetically, the direct bond cleavages should have steeper *k(E)* curves than does the elimination, which requires a tighter transition state (Chart 1). Hence, the direct bond cleavages are predicted to outcompete the HF elimination in dissociating $CHClF^\bullet$.

The thermochemical data (Tables 4 and 6) further predict the elimination of HCl to be the most favorable ion dissociation of $CHClF^+$. In accord with the dissociation energetics, the k_i values for elimination of HCl from $CHClF^+$ are uniformly greater than those for the more endothermic loss of $Cl^\bullet$ (Table 3). The branching ratio for HCl elimination and $Cl^\bullet$ loss, $k_i(HCl)/k_i(Cl)$, shows a minimum for neutralization with di-*n*-butylamine. This indicates that neutralization with the latter reagent, followed by reionization, produces the largest fraction of high-energy $CHClF^+$ ions. Although this is consistent with the overall greater extent of dissociation following neutralization with di-*n*-butylamine (Table 1), the rate parameters for dissociations of di-*n*-butylamine-neutralized $CHClF^\bullet$ *radicals* are comparable to those from neutralizations with the other targets. The fractions of competitive eliminations of HCl and HF from reionized $CHClF^+$ depend on the neutralization energetics (Table 3). In particular, the rate parameter for the elimination of HF from $CHClF^+$, which has a higher activation energy, increases with the neutralization exoergicity.

Discussion of the rate parameters for the neutral and ion dissociations raises the question of energy deposition in collisional neutralization at kiloelectronvolt collision energies, whose mechanism is not well understood.[15] The present analysis shows that the energy content in $CHClF^\bullet$ can be roughly composed of the precursor ion internal energy, which is limited from above by the lowest ion dissociation barrier of 346 kJ mol^{-1} (Table 6) and the Franck−Condon energy of ~34 kJ mol^{-1}, which combined are sufficient to promote cleavages of the C−H and C−Cl bonds in $CHClF^\bullet$. However, to account for the more endothermic dissociations (vide supra), a high-energy fraction of $CHClF^\bullet$ must be present, which acquired energy by the electron-transfer collision. It is noteworthy that the energy balance in the neutralization step has only a small effect on the internal energy in dissociating radicals. It may also be noted that collisional excitation of the intermediate radicals is also possible, although the probability for a second collision is only 15% at the 70% beam transmittance used.

Larger effects of ΔIE are observed on the dissociations of reionized ions, in particular for the competitive eliminations of HCl and HF. One possible interpretation of this phenomenon is that the various neutralization targets affect internal energy distribution in *nondissociating* $CHClF^\bullet$, especially those with internal energies close to the 306 kJ mol^{-1} threshold. If this fraction increases with increasing ΔIE, the internal energies in the reionized $CHClF^+$ will also shift to higher values and affect the ion dissociation kinetics. However, the internal energy deposition upon collisional reionization may depend on the internal energy of the intermediate neutral species,[36] which would further complicate the analysis. Although the present kinetic analysis does not yield any details of the internal energy distribution in $CHClF^\bullet$, the relative insensitivity of the neutral dissociations toward the ΔIE clearly indicates that the internal energy distribution in $CHClF^\bullet$ is broad and lacks pronounced minima or maxima.

Conclusions

The results obtained from the combination of variable-time neutralization−reionization mass spectrometry and ab initio calculations allow us to make the following conclusions. Fractions of stable $CHClF^\bullet$ and $CHCl_2^\bullet$ radicals are formed by vertical reduction of their respective cations. The dissociations of the intermediate radicals are distinguished from those of the reionized cations by the variable-time measurements. Loss of chlorine atom is a major unimolecular dissociation of $CHClF^\bullet$ and $CHCl_2^\bullet$ that occurs competitively on the microsecond time scale. It is concluded that $CHClF^\bullet$ radicals possessing >333 kJ mol^{-1} internal energy can serve as an efficient source of chlorine atoms and contribute to ozone depleting reactions.

Acknowledgment. Financial support by the National Science Foundation (Grant CHE-9412774) and the University of Washington Royalty Research Fund is gratefully acknowledged. Acknowledgments are also made to the donors of the Petroleum Research Fund, administered by the American Chemical Society, for support of this work. The ab initio computations were conducted by using the resources of the Cornell Theory Center, which receives major funding from the National Science Foundation and New York State with additional support from the Advanced Research Projects Agency, the National Center for Research Resources at the National Institutes of Health, IBM Corporation, and members of the Corporate Research Institute.

References and Notes

(1) Ravishankara, A.; Solomon, S.; Turnipseed, A. A.; Warren, R. F. *Science* **1993**, *259*, 194.

(2) (a) Warren, R.; Gierczak, T.; Ravishankara, A. R. *Chem. Phys. Lett.* **1991**, *183*, 403. (b) Gillotay, D.; Simon, P. C. *J. Atmos. Chem.* **1991**, *12*, 269. (c) Talukdar, R.; Mellouki, A.; Gierczak, T.; Burkholder, J. B.; McKeen, S. A.; Ravishankara, A. R. *J. Phys. Chem.* **1991**, *95*, 5815. (d) Wallington, T. J.; Hurley, M. D.; Shi, J.; Maricq, M. M.; Sehested, J.; Nielssen, O. J.; Elleremann, T. *Int. J. Chem. Kinet.* **1993**, *25*, 651. (e) Kaiser, E. W. *Int. J. Chem. Kinet.* **1993**, *65*, 667. (f) Zhang, Z.; Padmaja, S.; Saini, R. D.; Huie, R. E.; Kurylo, M. J. *J. Phys. Chem.* **1994**, *98*, 4312.

(3) Molina, M. J.; Rowland, F. S. *Nature* **1974**, *249*, 810.

(4) (a) Doucet, J.; Sauvageau, P.; Sandorfy, C. *J. Chem. Phys.* **1973**, *58*, 3708. (b) For a review see: Sandorfy, C. In *Chemical Spectroscopy and Photochemistry in the Vacuum-Ultraviolet*; Sandorfy, C., Ausloos, P. J., Robin, M. B., Eds.; Reidel: Dordrecht, 1974; pp 149−176.

(5) Lias, S. G.; Liebman, J. F.; Levin, R. D.; Kafafi, S. A. *NIST Standard Reference Database*, Version 2.01; National Institute of Standards and Technology: Gaithersburg, MD, Jan 1994.

(6) (a) Chang, H. W.; Setser, D. W.; Perona, M. J. *J. Phys. Chem.* **1971**, *75*, 2070. (b) Clough, P. N.; Polanyi, J. C.; Taguchi, R. T. *Can. J. Chem.* **1970**, *48*, 2919. (c) Kim, K. C.; Setser, D. W. *J. Phys. Chem.* **1974**, *78*, 2166. (d) Holmes, B. E.; Setser, D. W.; Pritchard, G. P. *Int. J. Chem. Kinet.* **1976**, *8*, 215. (e) Bogan, D.; Setser, D. W. In *Fluorine-Containing Free Radicals*, Root, J. W., Ed.; American Chemical Society: Washington, DC, 1978; Chapter 9, pp 237−280.

(7) Noble, D. *Anal. Chem.* **1993**, *65*, 693A.

(8) (a) Andrews, L.; Dyke, J. M.; Jonathan, N.; Keddar, N.; Morris, A. *J. Am. Chem. Soc.* **1984**, *106*, 299−303.

(9) Hudgens, J. W.; Johnson, R. D. III.; Tsai, B. P. *J. Chem. Phys.* **1993**, *98*, 1925.

(10) Prochaska, F. T.; Andrews, L. *J. Chem. Phys.* **1980**, *73*, 2651.

(11) (a) Kuhns, D. W.; Tran, T. B.; Shaffer, S. A.; Tureček, F. *J. Phys. Chem.* **1994**, *98*, 4845. (b) Kuhns, D. W.; Tureček, F. *Org. Mass Spectrom.* **1994**, *29*, 463.

(12) Holmes, J. L. *Mass Spectrom. Rev.* **1989**, *8*, 513.

(13) (a) Hop, C. E. C. A.; Holmes, J. L. *Int. J. Mass Spectrom. Ion Processes* **1991**, *104*, 213. (b) Tureček, F.; Gu, M.; Hop, C. E. C. A. *J. Phys. Chem.* **1995**, *99*, 2278. (c) Nguyen, V. Q.; Shaffer, S. A.; Tureček, F.; Hop, C. E. C. A. *J. Phys. Chem.* **1995**, *99*, 15454.

(14) (a) Feng, R.; Wesdemiotis, C.; Zhang, M.-Y.; Marchetti, M.; McLafferty, F. W. *J. Am. Chem. Soc.* **1989**, *111*, 1986. (b) Wesdemiotis, C.; McLafferty, F. W. *Chem. Rev.* **1987**, *87*, 485.

(15) Lorquet, J. C.; Leyh-Nihant, B.; McLafferty, F. W. *Int. J. Mass Spectrom. Ion Processes* **1990**, *100*, 465.

(16) Curtis, L. A.; Raghavachari, K.; Pople, J. A. *J. Chem. Phys.* **1993**, *98*, 1293.

(17) (a) Tureček, F.; Gu, M.; Shaffer, S. A. *J. Am. Soc. Mass Spectrom.* **1992**, *3*, 493. (b) Tureček, F. *Org. Mass Spectrom.* **1992**, *27*, 1087.

(18) Fitch, W. L.; Sauter, A. D. *Anal. Chem.* **1983**, *55*, 832.

(19) (a) Millington, D. S.; Smith, J. A. *Org. Mass Spectrom.* **1977**, *12*, 264. (b) Bruins, A. P.; Jennings, K. R.; Stradling, R. S.; Evans, S. *Int. J. Mass Spectrom. Ion Phys.* **1980**, *36*, 69.

(20) Cooks, R. G.; Beynon, J. H.; Caprioli, R. M.; Lester, G. R. *Metastable Ions*; Elsevier: Amsterdam, 1973.

(21) Frisch, M. J.; Trucks, G. W.; Head-Gordon, M.; Gill, P. M. W.; Wong, M. W.; Foresman, J. B.; Johnson, B. G.; Schlegel, H. B.; Robb, M. A.; Replogle, E. S.; Gomperts, R.; Andres, J. L.; Raghavachari, K.; Binkley, J. S.; Gonzalez, C.; Martin, R. L.; Fox, D. J.; DeFrees, D. J.; Baker, J.; Stewart, J. J. P.; Pople, J. A. *Gaussian 92, Revision C*; Gaussian Inc.: Pittsburgh, PA, 1992.

(22) Møller, C.; Plesset, M. S. *Phys. Rev.* **1934**, *46*, 618.

(23) Mayer, I. *Adv. Quantum Chem.* **1980**, *12*, 189.

(24) Schlegel, H. B. *J. Chem. Phys.* **1986**, *84*, 4530.

(25) Baczkay, G. B. *Chem. Phys.* **1981**, *61*, 385.

(26) Hehre, W. J.; Radom, L.; Schleyer, P. v. R.; Pople, J. A. *Ab Initio Molecular Orbital Theory*; Wiley: New York, 1986.

(27) Pople, J. A.; Head-Gordon, M.; Raghavachari, K. *J. Chem. Phys.* **1987**, *87*, 5968.

(28) Novak, I.; Cvitas, T.; Klasinc, L.; Gusten, H. *J. Chem. Soc., Faraday Trans. 2* **1981**, *77*, 2049.

(29) Other sets of harmonic vibrational frequencies of $CHClF^+$ have been reported in refs 8 and 9, which closely agree with those calculated in this work.

(30) Su, T.; Bowers, M. T. In *Gas Phase Ion Chemistry*; Bowers, M. T., Ed.; Academic Press: New York, 1979; Vol. 1, Chapter 3, p 87.

(31) Cordero, M. M.; Hauser, J. J.; Wesdemiotis, C. *Anal. Chem.* **1993**, *65*, 1594.

(32) Danis, P. O.; McLafferty, F. W. *Anal. Chem.* **1986**, *58*, 348.

(33) Shaffer, S. A.; Tureček, F.; Cerny, R. L. *J. Am. Chem. Soc.* **1993**, *115*, 12117.

(34) Danis, P. O.; McLafferty, F. W. *Anal. Chem.* **1986**, *58*, 355.

(35) Holmes, J. L.; Hop, C. E. C. A. *Org. Mass Spectrom.* **1991**, *26*, 476.

(36) Harnish, D.; Holmes, J. L. *Org. Mass Spectrom.* **1994**, *29*, 213.

(37) NR efficiencies of some of the fragments were measured and found to depend on the ion kinetic energy; e.g., for 8150 and 3800 eV the efficiencies ($\times 10^5$) were as follows: CCl (39, 4.2), CF (83, 12.4), HCl (131, 11), HF (10, 9).

(38) (a) McAdoo, D. J. *Mass Spectrom. Rev.* **1988**, *7*, 363. (b) Bowen, R. D. *Acc. Chem. Res.* **1994**, *24*, 364. (c) Longevialle, P. *Mass Spectrom. Rev.* **1992**, *11*, 157.

(39) (a) Wang, D.; Squires, R. B.; Farcasiu, D. *Int. J. Mass Spectrom. Ion Processes* **1991**, *107*, R7. (b) Tumas, W.; Foster, R. F.; Brauman, J. I. *J. Am. Chem. Soc.* **1988**, *110*, 2714.

(40) Dyke, J. M.; Lewis, A. E.; Morris, A. *J. Chem. Phys.* **1984**, *80*, 1382.

(41) Hepburn, J. W.; Trevor, D. J.; Pollard, J. E.; Shirley, D. A.; Lee, Y. T. *J. Chem. Phys.* **1982**, *76*, 4287.

(42) (a) Stevenson, D. P. *Discuss. Faraday Soc.* **1951**, *10*, 35. (b) McLafferty, F. W.; Tureček, F. *Interpretation of Mass Spectra*, 4th ed.; University Science Books: Mill Valley, CA, 1993; p 53.

(43) Miller, T. M. In *Handbook of Chemistry and Physics*, 71st ed.; Lide, G. R., Ed.; CRC Press: Boca Raton, FL, 1990; Chapter 10, pp 193−209.

JP952416I